CEMENTITIOUS PLUG SEAL/ROCK INTERFACE UNDER STATIC AND DYNAMIC LOADINGS

Khaled M. Mohamed
National Institute for Occupational Safety and Health, (NIOSH), Pittsburgh, Pennsylvania USA

Asmaa M. Yassien
Suez Canal University, Suez Egypt

Syd S. Peng
West Virginia University, Morgantown, WV USA

ABSTRACT

Seals are structures built in underground coal mines to isolate mined areas from active mine workings. Cementitious plug seals are made of foamed cements with compressive strength ranging from 100 to 600 psi. The stability of the cementitious plug seal is based on balancing the load applied to the face of the seal from the explosion against the shearing resistance at the seal/rock interface. Therefore, the properties of the seal/rock interface, such as stiffness, cohesion, friction, etc. are critical to determine the stability of a cementitious seal. The objective of this research is to estimate the cementitious seal/rock interface properties from full scale test results.

Prior to the Sago disaster in 2006, the National Institute for Occupational Safety and Health (NIOSH) conducted full-scale tests within the Lake Lynn Experimental Mine (LLEM) on various cementitious plug seals designed to meet or exceed the 20-psi horizontal static load requirements of the old 30 CFR[1] 75.335. Both static and dynamic loading tests were conducted. Using the static and dynamic loading test data (pressure and displacement) collected at LLEM, the static and dynamic properties of the plug seal/rock interface are back calculated and validated.

Fast Lagrangian Analysis of Continua in Three Dimensions (FLAC 3D) models were developed to simulate Celuseal[2] low-density cementitious seals subjected to both static and dynamic loadings. The static shear stiffness, normal stiffness, and cohesion for plug seal/rock interface are back calculated 115 psi/in, 230 psi/in, and 75 psi respectively. Furthermore, the back calculated properties have been validated. For a single case study, it was found that the plug seal/rock interface properties (normal and shear stiffness and cohesion) under dynamic loading are two-and-half times their values when it subjected to static loading. Additional explosion tests are required to validate the back calculated dynamic properties of the seal/rock interface.

1. INTRODUCTION

Current MSHA regulations require seals to resist design pressure-time curves with a peak explosion pressure of 50 or 120 psi and instantaneous rise time depending on the seal application [1]. In designing a structure to resist the explosion load, two broad failure mechanisms require consideration [2]. For thin structures where the thickness-to-height ratio is less than one quarter, beam or plate analysis applies. Failure usually originates as tensile failure at mid-span on the seal face opposite the applied explosion loading. For thick structures where the thickness-to-height ratio is greater than 1, a plug analysis applies. Failure occurs as shear either through the seal material itself, through the foundation rock, or along the seal-rock interface.

Cementitious seals are made of aerated (foamed) cements that are formed by incorporating foaming agents into the cement to create air bubbles. When the cement is mixed with the proper amount of air and water, it begins to gel within minutes of discharge and forms a non-toxic, non-combustible product. It cures to a final unconfined compressive strength ranging from 100 to 600 psi. The foamed cements for mining applications are designed to allow pumping distance greater than 1,000 ft [3].

Plug seals are usually built at mine locations where a seal will be subjected to roof-to-floor convergence. The seal material can absorb some entry closure without compromising the structural integrity of the seal [4]. The plug seals

---

[1] *Code of Federal Regulations*. See CFR in references.

[2] Mention of any company or product does not imply endorsement by the National Institute for Occupational Safety and Health (NIOSH).

are not designed to control the roof-to-floor convergence but to isolate the mined areas from the active mine workings.

Prior to the January 2006 Sago mine disaster, NIOSH researchers conducted full-scale explosion tests at the Lake Lynn Experimental Mine (LLEM) on a wide variety of cementitious seals designed to meet the requirements of the old 20-psi standard. The structural response and failure data obtained from these tests can serve as reference for the calibration and verification of numerical models of seal behavior at the 20-psi design level, which then enables more reliable structural analysis of seal designs that meet the new explosion design criteria of 50 psi and 120 psi [5].

Bounded with the accuracy of data collected from seal testing at LLEM, the objective of this research is to define the proper rock/seal interface properties, such as shear stiffness, normal stiffness, cohesion, etc. These properties are back calculated and validated using the structure response data of cementitious seal tests and FLAC 3D models.

2. PLUG SEAL/ROCK INTERFACE PROPERTIES UNDER STATIC AND DYNAMIC LOADINGS

For 4-in long samples (average shear area of 15.422 in^2) at a low normal stress of 10 psi, the shear stiffness of cementitious material/rock interface was measured [6]. It varied from 1,091 psi/in to 4,704 psi/in with an average of 2,304 psi/in. The applied shear rate to the peak resistance was 0.001 in/min Therefore, it can be assumed that the measured shear stiffness is static. The shear stiffness of jointed rock is a scale dependent property that decreases in magnitude as the sharing area (sample size) increases [7]. Therefore, the in-situ shear stiffness of plug seal/rock interface could be smaller than the laboratory values.

The authors are unaware of any published direct measurements or characterizations for the cementitious plug seal/rock interfaces under static or dynamic loading conditions. Therefore, the joint characteristics of fractured or jointed rocks will be applied to describe the plug seal/rock interface. The seal/rock interface can be defined by the linear Coulomb shear-strength criterion that limits shear force acting on the interface. The important properties for the plug seal/rock interface are: normal and shear stiffness, cohesion and friction angle. A brief description of normal and shear stiffness properties under both static and dynamic loadings follows.

The normal stiffness K_n is defined as the normal stress increment required for closure of a joint or fracture, at a given level of effective stress [7]. Shear stiffness K_s is defined as the average slope of the shear stress-displacement curve (Figure 1). Experimental measurements show that K_n is significantly larger than the shear stiffness K_s. Normal stiffness is not believed to be scale-dependent [7]. Shear stiffness depends on the peak shear strength and displacement at peak, both of which are scale dependent [7]. The static ratio of K_n/K_s will tend to rise with increasing block size. For 4-in long samples and at normal stress of 145 psi, it was found that the static K_n/K_s ratio varied from 5.7 to 132. The range of dynamic K_n/K_s ratio for 2-in diameter jointed samples in quartz monzonite was from 1.3 to 4.3 with a mean of 2.5 [7].

Ray [8] summarized some of the published data for the joint properties used by various researchers to simulate the brick-mortar interface and rock joints for various applications. He concluded that the average K_n/K_s (static) ratio used by these researchers in mining applications is 2.

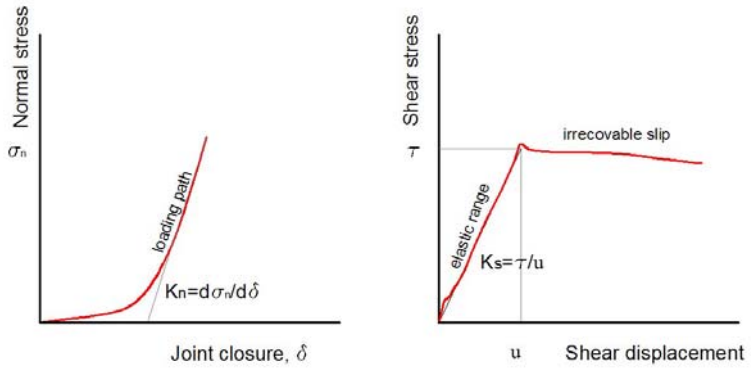

Figure 1. Normal and shear stiffness for jointed rock model

The testing results for jointed and/or fractured rocks indicated that K_s (dynamic) is likely to be some order of magnitude larger than K_s (static) at comparable normal stress levels [7]. The ratio of K_n (dynamic) to K_n (static) stiffness for fractured specimens of quartz monzonite specimens (2-in diameter x 3-in long) was 4.5, 3.6, and 7.6 for normal stresses of 420, 1450, and 4785 psi, respectively [9].

Shear tests of rock joints under both static and dynamic loading conditions were conducted by Barbero et al., [10] and Srivastava et al., [11]. Under low normal stress, the dynamic shear strength is greater than the corresponding static value and the dynamic shear strength is greater for higher rates of applied loading.

3. CEMENTITIOUS PLUG SEAL TESTS CONDUCTED AT LLEM

Examples of cementitious seals tested at LLEM are Tekseal by Minova, Celuseal by R.G. Johnson Company, and Ribfill seal and Rockfast seal by HeiTech Corporation [5]. A brief description of the static and dynamic test results for Celuseal plug structures will be presented in this study.

To make the 3D FLAC models comparable with the LLEM tests, only the experiments that assumed uniform pressure loading across the tested seal were selected. As described by Zipf [5], the following seal test loading conditions were used in LLEM tests:

1. Explosion tests with a reflected blast wave overpressure assumed to be relatively uniform across the seal face.
2. Hydrostatic chamber tests using water pressure that applied a static uniform loading across the seal face.
3. Hydrostatic chamber tests using a methane-ignition pressure that also applied a static uniform loading across the seal face.

4. CEMENTITIOUS PLUG SEAL SUBJECTED TO UNIFORM STATIC LOAD

Three statically-loaded cementitious plug seal structures were considered in this study. Table 1 shows the seal configuration and the critical parameters recorded in these tests. The first structure was statically loaded using the water pressure in the hydrostatic chamber. This structure was evaluated during three separate tests under similar test conditions. The second and third structures were loaded using the methane-ignition pressure in the hydrostatic chamber. The first structure was not damaged while the second and third structures were destroyed. The average compressive strength of the seal material was 350 psi [5]. No steel reinforcement or hitching to the surrounding rock was used in the construction of the tested seals. Pressure-time and displacement-time curves were recorded during these tests.

Table 1 Summary of seal structures subjected to static loadings [5]

Seal	Test #	Seal's dimensions			Average peak pressure, psi	Average displacement at peak, in	Observations
		Width, ft	Height, ft	Thickness, ft			
Structure 1	1	21.2	8.7	4	21.3	0.33	No damage
	2				30.6	0.46	No damage
	3				25.4	0.44	No damage
Structure 2	1	21.2	8.7	4	32.1	0.98	Destroyed
Structure 3	1	30.8	15.6	4	25.2	3	Destroyed

Three linear variable differential transducers (LVDTs) were used to measure the movement of the seals. The LVDTs were located at the center of the seal close to the bottom, middle and top of the seal surface. A strain gauge pressure transducer measured the water pressure behind the seal. Figures 2 to 4 show the pressure and displacement histories for the three tests conducted on structure 1. These figures show the recorded histories up until the time the water pump was stopped. The descending portions of the curves correspond to the drop in pressure related to the water drainage from behind the seal and were therefore omitted from these figures.

Figures 5 and 6 show the average pressure and average displacement histories for structures 2 and 3, respectively. The static load on these structures was induced by a methane ignition within the confined chamber behind the structure. The data shows the displacements increase rapidly just before the seals fail.

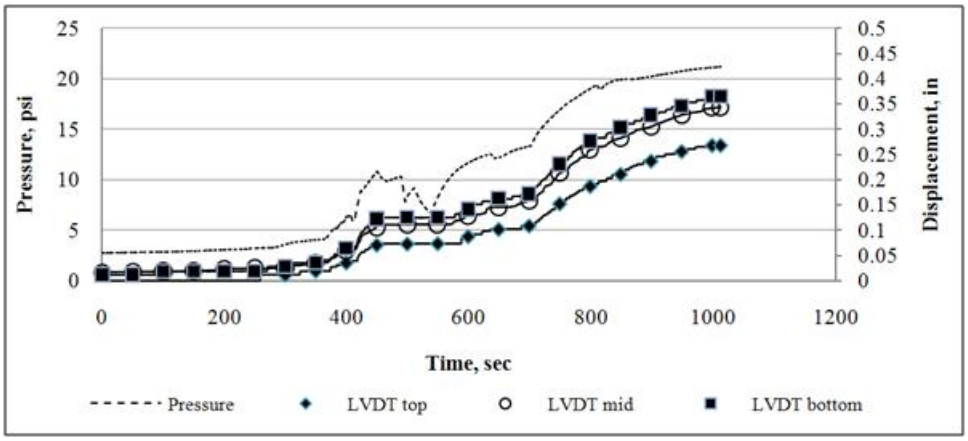

Figure 2. Applied pressure and seal displacement history curves for structure 1, test 1 as evaluated within the hydrostatic chamber [5]

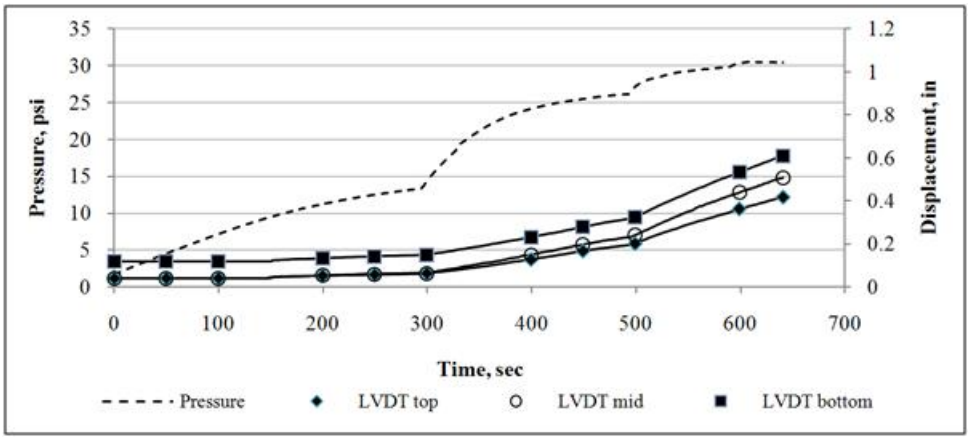

Figure 3. Applied pressure and seal displacement history curves for structure 1, test 2 as evaluated within the hydrostatic chamber [5]

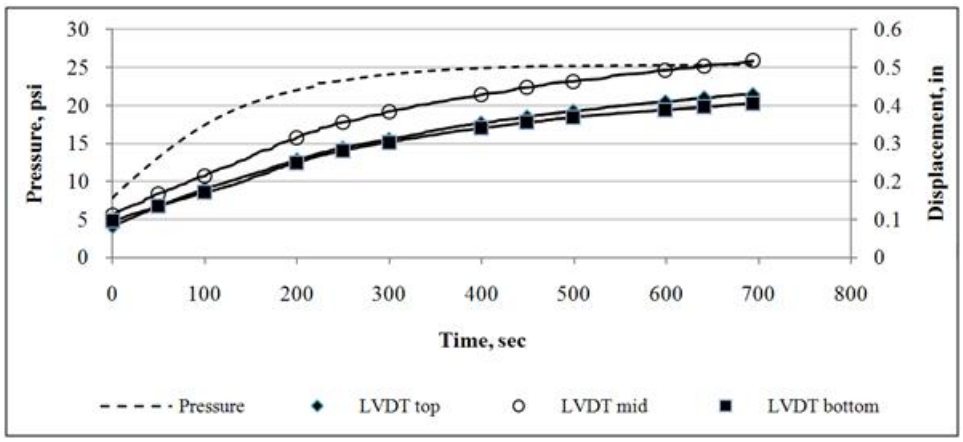

Figure 4. Applied pressure and seal displacement history curves for structure 1, test 3 as evaluated within the hydrostatic chamber [5]

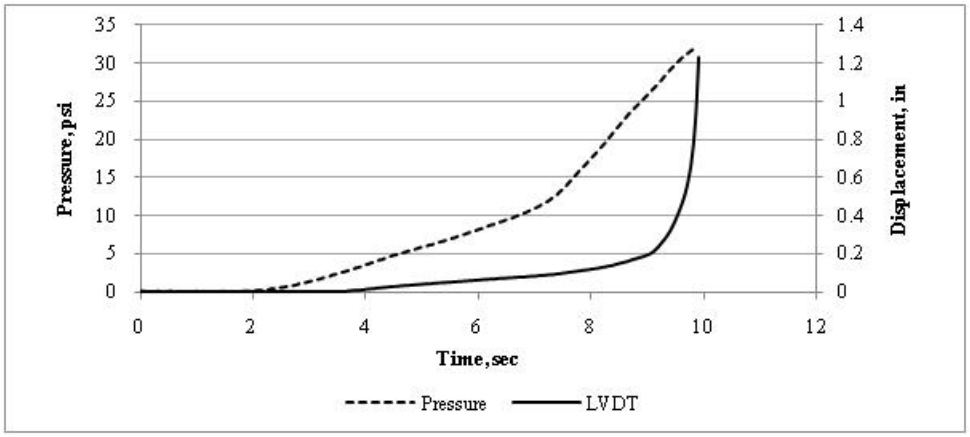

Figure 5. Applied pressure and seal displacement history curves for structure 2 as evaluated within the hydrostatic chamber [5]

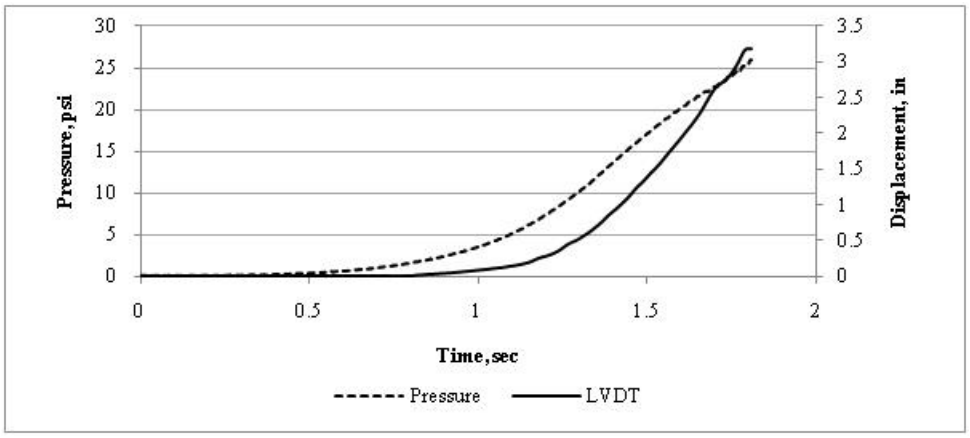

Figure 6. Applied pressure and seal displacement history curves for structure 3 as evaluated within the hydrostatic chamber [5]

4.1 ESTIMATION OF THE STATIC PROPERTIES OF SEAL/ROCK INTERFACE

The test results for structure 1 enable estimating of the static shear stiffness and cohesion of the seal/rock interface. The shear displacement is estimated as the average of the top, middle and bottom LVDTs readings. The shear stress, τ_s is estimated as follows:

$$\tau_s = \frac{P \times W \times H}{2 \times (W + H) \times T} \tag{1}$$

where

T is the thickness of the seal (4 ft),
W is width of the seal (21.2 ft),
H is height of the seal (8.7 ft),
P is the applied pressure.

Figure 7 shows the derived relationship between the estimated seal/rock shear stress and the shear displacement for structure 1, tests 1, 2, and 3. The shear stiffness of the seal/rock interface is estimated by the slope of the relationship between the shear stress and shear displacement operating at the interface. From figure 7, the static shear stiffness of the seal/rock interface for structure 1 ranges from 65 to 173 psi/in.

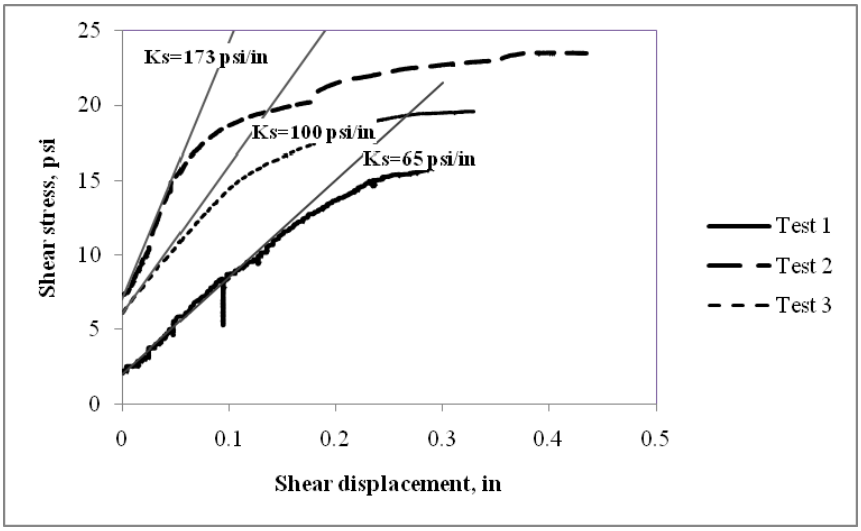

Figure 7. Seal/rock interface shear stress vs. shear displacement for structure 1, tests 1, 2, and 3 as evaluated within the hydrostatic chamber

4.2 FLAC 3D SEAL MODEL

Fast Lagrangian Analysis of Continua in Three Dimensions [12] (FLAC 3D) models were developed to simulate plug seals subjected to both static and dynamic loadings. Figure 8 shows the configuration of the FLAC 3D model for the structure 1. The left and right sides are constrained in the x-direction. The front and back sides are constrained in the y-direction. The bottom and top sides are constrained in the z-direction. Figures 2 to 4 show that structure1 was subjected to a state of static loading because of the long duration of the applied pressure (650-1000 sec). To simulate the explosion or water pressure applied on the seal, the inby side of the seal was uniformly loaded by static pressure in the positive y-direction.

The Mohr-Coulomb model was used to simulate the seal material. Since LLEM is a limestone mine, elastic properties of limestone were assigned for the roof, floor and ribs. The foundation conditions for seal structures constructed and tested at LLEM can be described as “rigid” or “unyielding” [5]. Table 2 shows the material properties of seal and the surrounding rock.

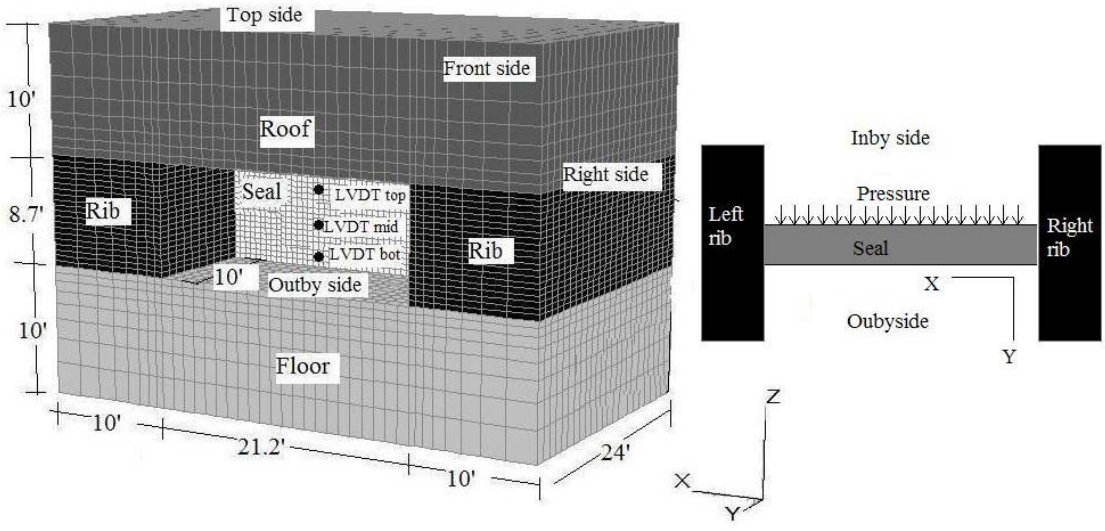

Figure 8. Three-dimension model for the cementitious seal

Table 2 Material properties used in the model

Material	Young's modulus, $x10^6$ psi	Poisson's ratio	Compressive strength, psi	Cohesion, psi	Friction angle, deg	Tensile strength, psi
Limestone	2.5	0.3	-	-	-	-
Cementitious seal	0.21	0.26	350	112	24.5	89

Because the tests at LLEM were conducted with no roof-to-floor convergence applied on the seal, the friction component of the seal/rock interface is ignored. Therefore the friction angle was assumed to be zero. This assumption is valid as long as the shear displacement of seal/rock interface is in elastic range (Figure 1) and the seal is not hitched to the surrounding rocks. These conditions are completely applicable for structure 1 which was used to back calculate the seal/rock interface. The joint shear stiffness is independent of the applied normal stress [13]. Therefore, even if there was an induced normal stress on the seal/rock interface, because of the seal loading, it wouldn't affect the back calculated shear stiffness of that interface. The static normal stiffness (K_n) of the seal/rock interface was assumed to be two times the static shear stiffness (K_s) [8]. The maximum shear stresses (23.5 psi) recorded in Figure 7 should be smaller than the static interface cohesion because none of the three tests on structure 1 reached the ultimate capacity of the seal. Table 3 shows the estimated ranges of the static seal/rock interface properties. Using FLAC 3D models, the static stiffness and cohesion for the seal/rock interface will be back calculated and validated using the experimental results shown in Figures 2 to 4.

Table 3. Static seal/rock interface properties

	Shear stiffness, K_s psi/in	Normal stiffness, K_n psi/in	Cohesion, C_{int} psi
Estimated range	$65 < K_s < 173$	$130 < K_n < 346$	$23.5 < C_{int} < \tau$

τ is the shear strength for the seal material (τ = 112 psi).

4.3 BACK CALCULATION OF THE SEAL/ROCK INTERFACE STATIC PROPERTIES

Structure 1, test 2 was used to back calculate the static properties of the seal/rock interface. The model shown in Figure 8 was used to simulate the loading condition for structure 1 test 2. A uniform pressure of 30.6 psi was applied on the inby side of the seal and the lateral displacements at the bottom, middle and top of the outby side of the seal were recorded. Based on the experimental results, estimated ranges for the static shear stiffness of the seal/rock interface was determined (Table 2). The static shear stiffness of the seal/rock interface is back calculated by estimating the lateral displacements for structure 1, test 2 assuming different values of the interface shear stiffness. The predicted displacements were compared with the measured ones at the middle and bottom of the seal. The interface normal stiffness was taken as two times the shear stiffness [8]. Two levels of interface cohesion were considered in the back calculation, i.e., 50 and 75 psi.

Figures 9 and 10 show the predicted displacements at the middle and bottom of the outby side of the seal for different interface shear stiffness. The static cohesion has no effect on the predicted lateral displacement of the seal. The static shear stiffness has obvious effect on the seal response. Greater stiffness results in lower seal lateral displacement. An interface shear stiffness of 115 psi/in shows lateral displacements close to the measured ones. The estimated middle and bottom lateral displacements for an interface shear stiffness of 115 psi/in are 0.48 and 0.47 in, respectively. The measured displacements were 0.45 and 0.55 in. at the middle and bottom of the seal, respectively.

The back calculated seal/rock shear stiffness (115 psi/in) is approximately twenty times less than the average shear stiffness (2,304 psi/in) obtained from the laboratory scale shear tests [6]. This significant reduction in the in-situ shear stiffness for the seal/rock interface is due to the in-situ shearing area (34,400 in^2) being much greater than the laboratory shearing area (15.422 in^2). The back calculated static shear stiffness, normal stiffness, and cohesion for seal/rock interface are 115 psi/in, 230 psi/in, and 75 psi, respectively.

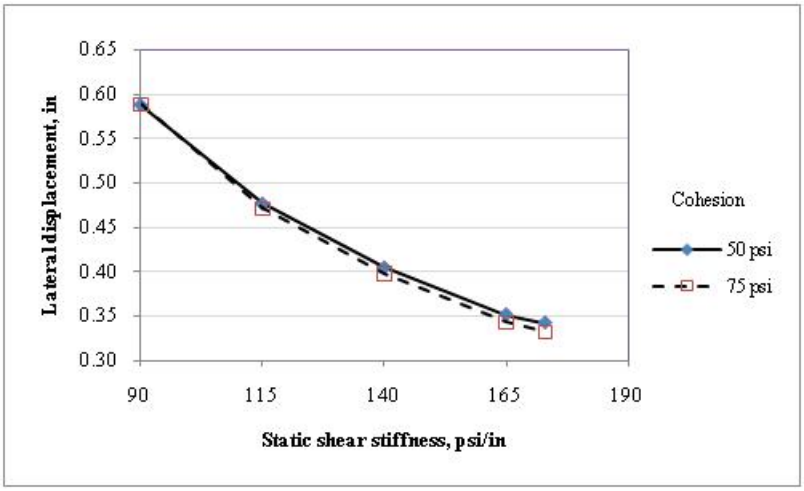

Figure 9. Effect of the static shear stiffness of the seal/rock interface on the predicted displacement at the middle of the seal for structure 1, test 2

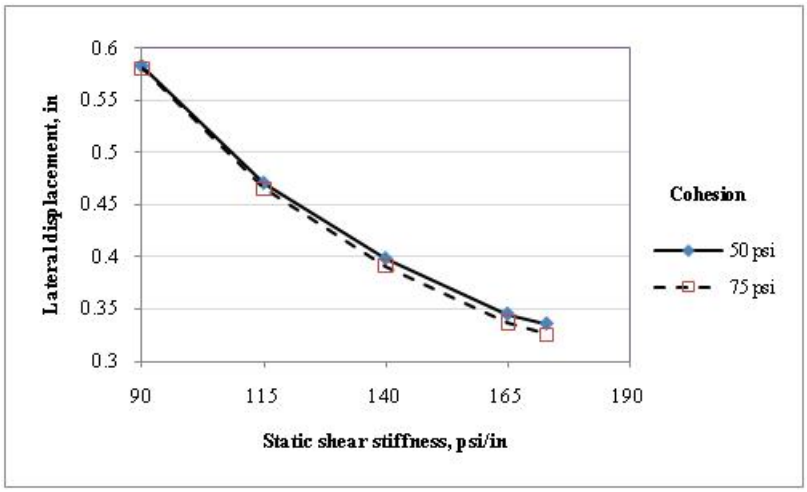

Figure 10. Effect of the static shear stiffness of the seal/rock interface on the predicted displacement at the bottom of the seal for structure 1, test 2

4.4 VALIDATION OF THE SEAL/ROCK INTERFACE STATIC BACK CALCULATED PROPERTIES

The back calculated properties of the seal/rock interface properties were validated using test results of structure 1 (1 tests 1and 3), structure 2 and structure 3. The modeling methodology described earlier was used to simulate the loading conditions for un-damaged structure 1 (tests 1 and 3) and damaged structures 2 and 3.

Figures 11 and 12 show the predicted and measured displacements at the middle and bottom of the structure1, respectively. Because of the seal symmetry, the predicated top and bottom displacements are identical. Therefore, Figure 12 shows only the predicted displacement at the top of the seal. The measured top and bottom displacements are averaged and compared with the predicted top displacement (Figure 12). Except for the middle displacement for structure 1, test 3, the models are able to predict the seal lateral displacements with sufficient accuracy.

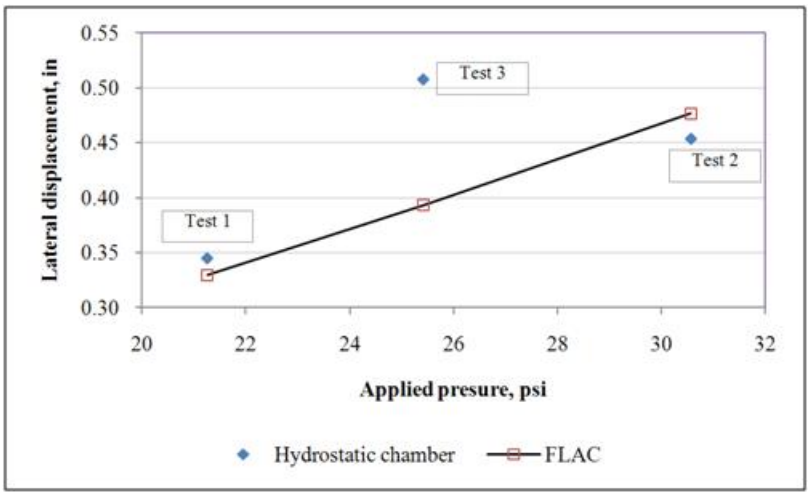

Figure 11. Predicted and measured displacements at the middle of the seal (structure 1). The measured displacements were from the seal evaluations within the hydrostatic chamber

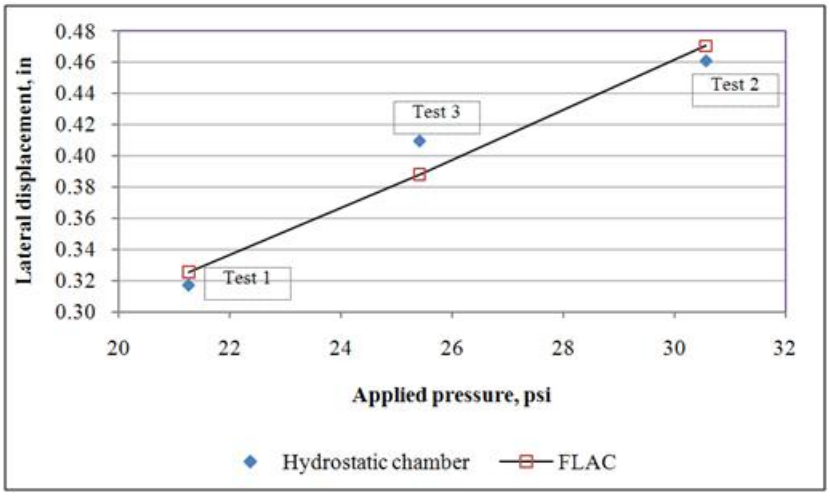

Figure 12. Predicted and average measured displacements at the top and bottom of the seal (structure 1). The measured displacements were from the seal evaluations within the hydrostatic chamber

The FLAC 3D model for structure 2 predicts lateral seal displacement of 0.492 in. In the last second before the peak pressure, the actual measured displacement for structure 2 during the test (Figure 5) increased rapidly from 0.2 in to 1.0 in. The predicted seal displacement for structure 2 at the peak pressure is within the recorded displacement range during the test.

The FLAC 3D model for structure 3 predicts lateral seal displacement of 1.319 in. Similar to structure 2, in the last second before the peak, the measured displacement (Figure 6) increased rapidly from 0.5 in to 3.0 in. The predicted seal displacement for structure 3 at the peak pressure is within the recorded displacement range.

Figure 13 shows the yielding state for structure 1, test 2 as predicted by the FLAC 3D model. Blue elements indicate that the state of stress in these elements is in the elastic range while any other colored elements indicate that these elements are yielded (damaged). Figure 13 shows tensile yielding in the outby side of the seal. This tensile failure is localized in the middle of the seal for a distance of 6 in. The models for structure 1, tests 1 and 3 predicted elastic state of stresses in these tests. Structure 1, tests 1 and 3 show no damage during the test (Table 1). Hence, the predicted yielding conditions for structure 1, tests 1 and 3 matches with test observations of structure 1.

Figure 14 shows the yielding state for structure 2 as predicted by the FLAC 3D model. Tensile yielding occurs on the outby side of the seal. This tensile failure is localized in the middle of the seal for a distance of 6 in. Structure 2

shows damage during the test (Table 1). The predicted yielding conditions for structure 2 match well with damage observations during the tests.

Figure 15 shows the yielding state for structure 3 as photographed during the test and predicted by the model. Both the test photograph and the model show tensile failure at the middle of the outby side of the seal. Structure 3 shows damage during the test (Table 1). The predicted yielding conditions for structure 3 match with test observations for structure 3.

The predicted lateral displacements and damage conditions for structures 1, 2 and 3 indicates that the back calculated seal/rock interface properties could represent the actual behavior of the static cementitious plug seal/rock interface during the LLEM tests. Table 1 shows that these tests were conducted under both water and gas pressure loadings. It was hypothesized that loading the seal structure by water pressure could lead to reduction of the shear stiffness of the seal/rock interface. The modeling and testing results for structure 1 (water loaded) and structures 2 and 3 (methane-ignition loaded) show that loading the seal structure by water or methane-ignition has no significant effect on the behavior of the seal/rock interface.

The back calculated static properties of cementitious seal/rock should help in the design of the cementitious plug seals. The seal can be statically designed to at least twice the expected dynamic performance pressure to meet the current MSHA regulations for seal design [14].

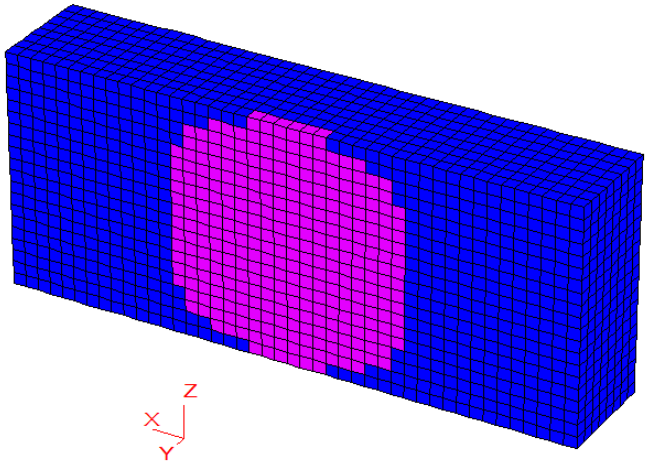

Figure 13. Yielding condition contours for structure 1, test 2 in the outby side of the seal

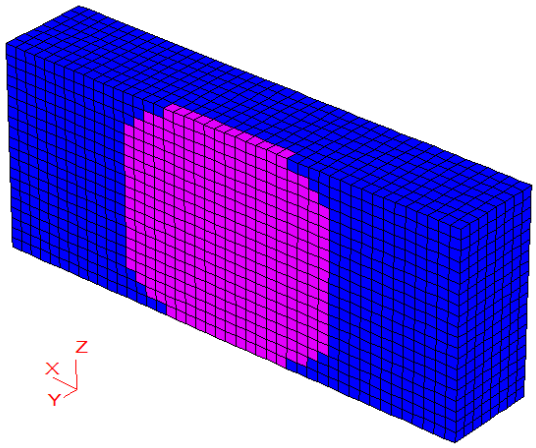

Figure 14. Yielding condition contours for structure 2 in the outby side of the seal

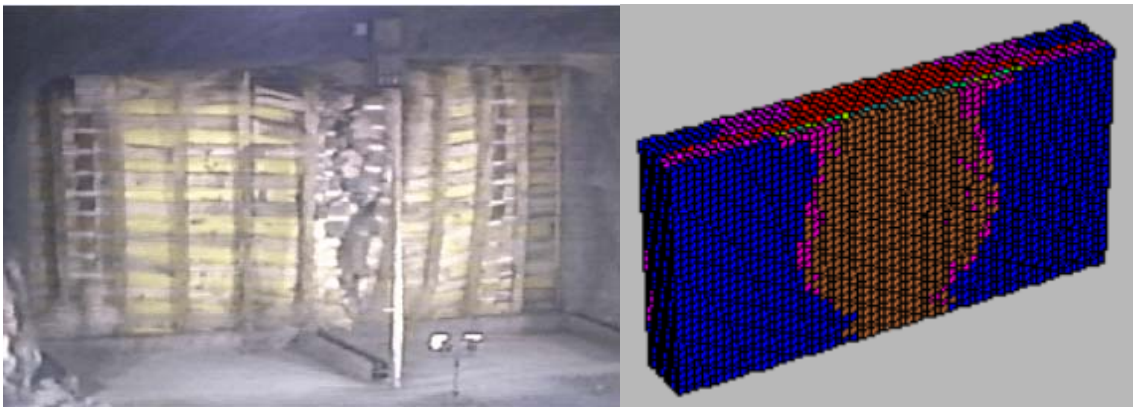

(a) In-situ (b) Model

Figure 15. Yielding condition contours for structure 3 in the outby side of the seal

5. CEMENTITIOUS PLUG SEAL SUBJECTED TO UNIFORM DYNAMIC LOAD

The cementitious plug seal (structure 4) selected to represent seals under dynamic loading was 5.1-ft thick, 18.7-ft wide, and 7.3- ft high. The tested seal was constructed perpendicular to the axis of the experimental drift and at distance of 320 ft from the ignition zone [14] and then subjected to a confined methane-air explosion (Figure 16). The pressure history was recorded 1 ft in front of the test seal while the seal displacement was recorded with a LVDT at the middle of the outby side of the seal. Figure 17 shows that the peak pressure applied on the seal for structure 4 was 60 psi with rise-up time of 0.01 sec and within 0.3 sec the pressure decayed to be less than 5 psi. Within 0.02 sec, the seal lateral displacement reached its peak of 0.6 in. then decayed to 0.4 in. in 0.28 sec.

The average compressive strength of the seal material was 143 psi [5]. Steel reinforcement and hitching to the surrounding rock were not used in the initial construction of this cementitious plug-type seal [5]. However prior to the explosion test, a 13-in-thick retrofit structure utilizing a solid-concrete-block wall, polyurethane, carbon fiber-reinforced polymer reinforcement, and heavy steel angle iron reinforcement to the mine floor and roof (simulated hitching) was installed against the cementitious plug-type seal on the outby side [15]. The purpose of this retrofit was to strengthen the cementitious seal which was designed to withstand 20 psi overpressure.

The test conducted on structure 4 is the only dynamic experiment that has both pressure and displacement data [5]. Therefore, despite of the complex nature of structure 4, it was used to back calculate the cementitious seal/rock interface properties under dynamic load.

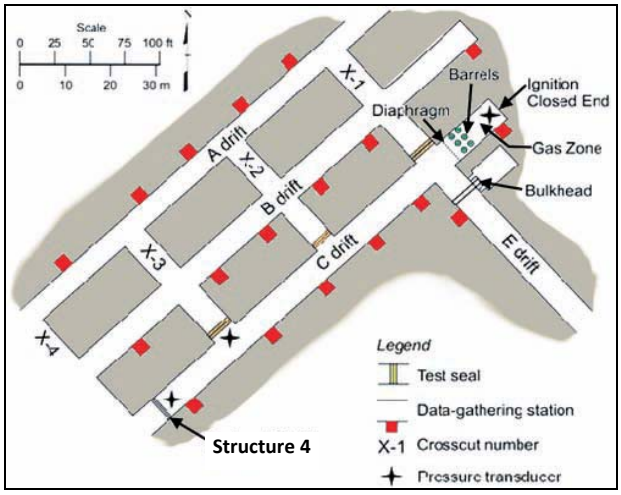

Figure 16. Test site for structure 4 [14]

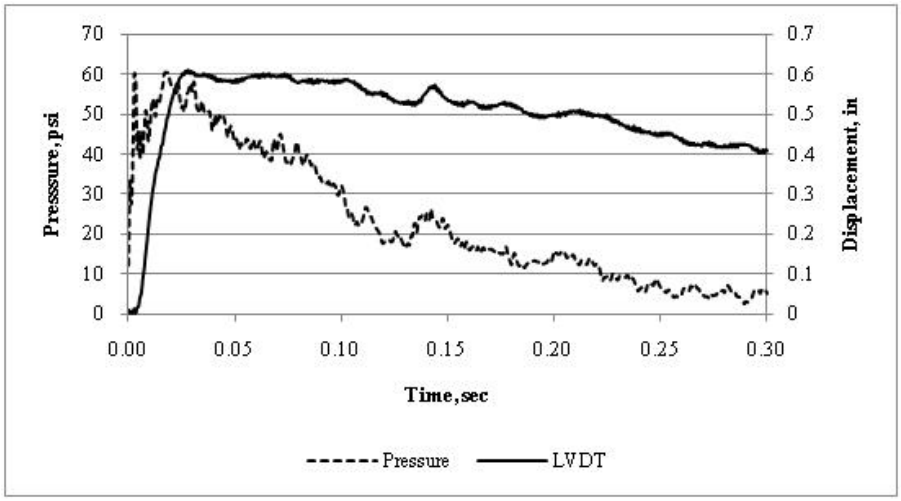

Figure 17. Applied pressure and seal displacement history curves for structure 4 as evaluated during a confined explosion test within the LLEM [5]

5.1 ESTIMATION OF THE PROPERTIES OF DYNAMIC SEAL/ROCK INTERFACE

The explosion for structure 4 (Figure 16) was used to back calculate the dynamic seal/rock interface properties. A FLAC 3D dynamic model to simulate structure 4 was developed (Figure 18). To simply consider the hitching effect of heavy steel angle used in the test, a row of rock elements was created against the outby side of the seal at the bottom and the top of the seal (Figure 18). The boundary conditions used to model structures 1 to 3 were used in structure 4, except that the measured pressure-time of Figure 17 was applied on the inby side of the seal. To dampen seal motion after reaching peak displacement, a local damp of 1.5% of critical damp was applied in the model. For geological materials, damping commonly falls in the range of 2 to 5% of critical [11].

The strength properties of structure 4 were assumed to be three times the values used for structures 1, 2 and 3 (Table 2). This assumption was made to match the non-damaged test results and the effect of the installed retrofit.

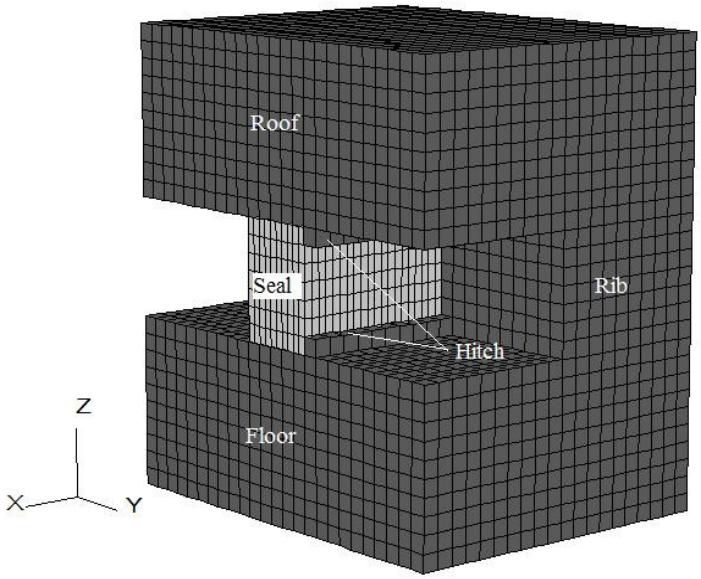

Figure 18. Three-dimension half-model for the structure 4

As explained earlier, the dynamic properties of the seal/rock interface are expected to be some order larger than that of the static properties at comparable normal stress levels [7]. To back calculate the dynamic properties of the seal/rock interface for structure 4, three levels (2, 2.5 and 3 times of the static seal/rock interface properties) were tried. Both of the interface stiffness (normal and shear) and cohesion were changed simultaneously.

Figure 19 shows the predicted lateral displacement histories at the middle of the outby side of the seal. It shows that a good agreement between the predicted and measured lateral displacements occurs when the dynamic seal/rock interface properties are two-and-half times that of the static properties. Additional explosion tests are required to validate the back calculated dynamic properties of the seal/rock interface.

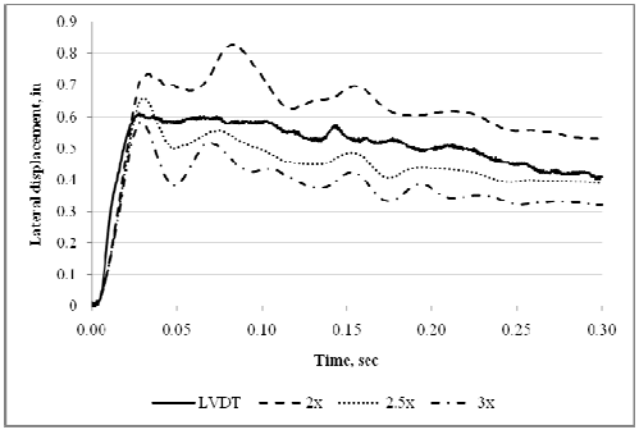

Figure 19. Predicted and measured lateral displacement for structure 4. The measured displacements were from the seal at confined explosion test within the LLEM

6. CONCLUSIONS

Cementitious plug seals are built in underground coal mines to isolate mined areas from active mine workings. The stability of the cementitious plug seal is based on balancing the load applied to the face of the seal from the explosion against the shearing resistance at the seal/rock interface. The objective of this research is to estimate the cementitious seal/rock interface properties from full scale test results.

Numerical modeling could be the best approach to predict the response of cementitious plug seals subjected to static or dynamic loadings. In order to have realistic numerical simulation for the cementitious plug seals, the seal/rock interface must be considered in the simulation. Bounded with the accuracy of data collected from seal tests at LLEM, the in-situ static and dynamic seal/rock interface properties (stiffness, cohesion, etc) were back calculated from these tests.

The back calculated static shear stiffness, normal stiffness, and cohesion for seal/rock interface are 115 psi/in, 230 psi/in, and 75 psi, respectively. Furthermore, the estimated properties have been validated by the tests conducted in the hydrostatic chamber. The back calculated in-situ seal/rock shear stiffness (115 psi/in) is approximately twenty times less than the average shear stiffness (2,304 psi/in) obtained from the laboratory scale shear tests

The back calculated static properties of cementitious seal/rock should help in the design of the cementitious plug seals. The seal can be statically designed to at least twice the expected dynamic performance pressure to meet the current MSHA regulations for seal design.

For a single case study, the dynamic properties of the seal/rock interface were back calculated. Additional explosion tests are required to validate the back calculated dynamic properties of the seal/rock interface.

ACKNOWLEDGEMENT

This work was sponsored by the National Institute for Occupational Safety and Health (NIOSH) – Pittsburgh Research Laboratory through Contract No. 2007-N-09921, Dr. Karl Zipf, Project Officer. This research was performed prior to the senior author joining NIOSH.

DISCLAIMERS

The findings and conclusions in this report are those of the authors and do not necessarily represent the views of the National Institute for Occupational Safety and Health. Mention of any company or product does not imply endorsement by NIOSH.

REFERENCES

1. Federal Register, (2008). "Rules and regulations sealing of abandoned areas-final rule," Title 30 CFR Part 75.335 CFR, Code of Federal Regulations, Washington DC: U.S. Government Printing Office, Office of the Federal Register 73(76), April 18, 2008.
2. Zipf, R. K., Brune, J. F. and Thimons, E. D., (2009). "Progress Toward Improved Engineering of Seals and Sealed Areas of Coal Mines", SME Annual Meeting, Denver, CO, Preprint 09-102.
3. Barczak, T. M. and Tadolini, S. C, (2005). "Pumpable roof supports: an evaluation in longwall roof support technology", www.cdc.gov/niosh/mining/pubs/pdfs/prsae.pdf.
4. Gadde, M. M., Beerbower, D., Rusnak, J., Honse, J.Worley, P., (2007). "Post-PIB P06-16: How to design alternative mine seals?" Paper presented at the SME annual meeting, Denver, CO, SME Pre-print No. 07-138.
5. Zipf, R. K., Weiss, E. S., Harteis, S. P. and Sapko, M. J., (2009). "Compendium of structural testing data for 20-psi coal mine seals", NIOSH Information Circular/ 9515.
6. Peng, S. S., 2009, "Personal communication"
7. Barton, N., (2007). "Rock quality, seismic velocity, attenuation and anisotropy", Taylor & Francis Group, London, UK, pp. 492, 497, 489 and 499.
8. Ray, A. K., (2009). " Influence of cutting sequence and time effects on cutters and roof falls in underground coal mine – numerical approach" Ph D Dissertation, WVU, pp. 12 -125.
9. Pyrak-Nolte, L. J. and Cook, N. G. W., (1987). "Seismic visibility of fractures", 28th US Symposium on Rock Mechanics, Tucson, pp. 47-56.
10. Barbero, M., Barla, G. and Zaninetti, A., (1996). "Dynamic shear strength of rock joints subjected to impulse loading", International Journal of Rock Mechanics and Mining Science & Geomechanics Abstracts, Vol. 33, No. 2, pp. 141-151.
11. Srivastava, V., Shukla, A. and Parameswaran, V., (2000). "Experimental evaluation of the dynamic shear strength of adhesive-bond lap joints", Journal of Testing and Evaluation, Vol. 28, No.6, pp. 438-442.
12. Itasca Consulting Group, Inc., (2006). "Fast Lagrangian Analysis of Continua in 3 Dimensions, FLAC3D Version 3.1)", Manual, Minneapolis, USA.
13. Jaeger, J.C., Cook, N.G. and Zimmerman, R. W., (2007), "Fundamentals of rock mechanics", Fourth ed., Blackwell Publishing, pp. 376.
14. Sapko, M. J., Harties, S. P., and Weiss, E. S., (2008). "Comparison of methods: dynamic versus hydrostatic testing of mine ventilation seals", Mining Engineering, Vol. 60, No. 9, pp 147-153.
15. Weiss, E. S. and Harteis, S. P., (2008). "Strengthening existing 20-psi mine ventilation seals with carbon fiber-reinforced polymer reinforcement", Pittsburgh, PA: U.S. Department of Health and Human Services, Public Health Service, Centers for Disease Control and Prevention, National Institute for Occupational Safety and Health, DHHS (NIOSH) Publication No. 2008-106, RI 9673.